

Richard Fritzsche

Robust Signal Processing for Cooperative Multi-Cell Transmission



Beiträge aus der Informationstechnik

Mobile Nachrichtenübertragung

Nr. 67

**Richard Fritzsche**

**Robust Signal Processing for  
Cooperative Multi-Cell Transmission**

 VOGT

Dresden 2014

Bibliografische Information der Deutschen Bibliothek

Die Deutsche Bibliothek verzeichnet diese Publikation in der Deutschen Nationalbibliografie; detaillierte bibliografische Daten sind im Internet über <http://dnb.ddb.de> abrufbar.

Bibliographic Information published by the Deutsche Bibliothek

The Deutsche Bibliothek lists this publication in the Deutsche Nationalbibliografie; detailed bibliographic data is available in the internet at <http://dnb.ddb.de>.

Zugl.: Dresden, Techn. Univ., Diss., 2014

Die vorliegende Arbeit stimmt mit dem Original der Dissertation

„Robust Signal Processing for Cooperative Multi-Cell Transmission“ von Richard Fritzsche überein.

© Jörg Vogt Verlag 2014

Alle Rechte vorbehalten. All rights reserved.

Gesetzt vom Autor

ISBN 978-3-938860-74-8

Jörg Vogt Verlag  
Niederwaldstr. 36  
01277 Dresden  
Germany

Phone: +49-(0)351-31403921

Telefax: +49-(0)351-31403918

e-mail: [info@vogtverlag.de](mailto:info@vogtverlag.de)

Internet : [www.vogtverlag.de](http://www.vogtverlag.de)

TECHNISCHE UNIVERSITÄT DRESDEN

# Robust Signal Processing for Cooperative Multi-Cell Transmission

Richard Fritzsche

von der Fakultät Elektrotechnik und Informationstechnik  
der Technischen Universität Dresden

zur Erlangung des akademischen Grades eines

**Doktoringenieurs**

(Dr.-Ing.)

genehmigte Dissertation

Vorsitzender Prof. Dr.-Ing. habil. Udo Jörges  
Gutachter Prof. Dr.-Ing. Dr. h.c. Gerhard P. Fettweis  
Prof. Dr. rer. nat. Rudolf Mathar

Tag der Einreichung: 07. April 2014  
Tag der Verteidigung: 16. Juli 2014



# Abstract

The requirements on throughput per area in cellular communications are steadily increasing due to the growing demand for multimedia applications. This challenge can basically be overcome by higher bandwidths, smaller cells as well as an increase in resource utilization, in terms of higher spectral efficiency. The first two approaches typically come with large financial investments due to the costs of rights to use radio frequencies, or the installation of additional base stations. An increase in spectral efficiency can be achieved by using new technologies. As of today, multi-antenna systems lead to significant gains in the performance of mobile communication networks. In this regard, spatial degrees of freedom can be exploited by shaping interference beneficially and transmitting multiple data streams in parallel using the same radio resource. The original concept includes co-located antenna arrays in combination with spatial signal processing on transmitter and receiver side. The limited size of mobile devices makes it beneficial to extend the multi-antenna concept to point-to-multi-point applications, with distributed non-cooperative user equipments, by shifting the spatial signal processing to the base station side. The downlink direction is particularly challenging, since interference between multiple users needs to be processed jointly before transmission. This pre-processing (precoding) requires channel state information (CSI) at the base station site, which is made available via feedback in frequency division duplex systems. The extension to multi-point-to-multi-point systems is achieved by coupling the antennas of multiple base stations virtually to increase the number of data streams transmitted in parallel. This technique requires additional signal processing effort as well as an increased amount of user data and CSI exchanged between base stations.

While theory provides significant gains for cooperative multi-cell transmission, the performance of practical systems suffers from impaired CSI due to, e.g., noisy pilot reception, quantization, and delays in feedback transmission and backhaul exchange. Although, backhaul latency can be reduced by replacing the infrastructure, large investments are required.

This work provides an alternative approach which bears infrastructural imperfections by reducing the impact of impaired channel knowledge with robust signal processing. In this regard, a two-step approach is presented. First the quality of CSI is increased and second, advanced precoding techniques which exploit statistical side information of the channel uncertainty are introduced. A major aspect of this work pertains to techniques and requirements for distributed precoding, which has the potential to provide significant gains compared to centralized precoding.

# Zusammenfassung

Der Bedarf an Datendurchsatz pro Fläche steigt in zellularen Mobilfunknetzen aufgrund wachsender Ansprüche an multimediale Anwendungen stetig. Diese Herausforderung kann durch mehr Bandbreite, kleinere Mobilfunkzellen sowie einer höheren spektralen Effizienz bewältigt werden. Die ersten beiden Ansätze sind in der Regel mit erheblichen finanziellen Aufwendungen durch den Erwerb von Frequenznutzungsrechten oder der Installation neuer Basisstationen verbunden. Die Erhöhung der spektralen Effizienz kann durch den Einsatz von Mehrantennensystemen erfolgen, welche bereits heute für deutliche Leistungsgewinne in mobilen Funkstandards sorgen. Hierbei können räumliche Freiheitsgrade ausgenutzt werden um Interferenz gewinnbringend zu verformen und mehrerer Datenströme auf der selben Funkressource parallel zu übertragen. Das ursprüngliche Konzept beinhaltet lokale Antennenfelder sowie räumliche Signalverarbeitung auf Sende- und Empfangsseite. Durch die begrenzte Größe mobiler Endgeräte ist es vorteilhaft das Konzept auf Punkt-zu-Mehrpunkt Anwendungen mit nicht kooperierenden Empfängern zu erweitern. Dabei muss die räumliche Signalverarbeitung auf die Basisstationsseite verschoben werden. Die Abwärtsstrecke ist besonders herausfordernd, da Interferenz zwischen Nutzern gemeinsam vor der Übertragung verarbeitet werden muss. Diese Vorverarbeitung (Vorverzerrung) benötigt Kanalzustandsinformationen (CSI) auf basisstationsseite, welche durch Feedback verfügbar gemacht wird. Die Erweiterung zu Mehrpunkt-zu-Mehrpunkt Systemen wird durch die virtuelle Kopplung der Antennen mehrerer Basisstationen erreicht, wodurch die Anzahl an parallel übertragenen Datenströmen gesteigert werden kann. Diese Technik erfordert neben zusätzlichem Signalverarbeitungsaufwand einen erhöhten Austausch von Nutzerdaten und CSI zwischen den Basisstationen.

Während theoretisch hohe Gewinne durch kooperative Übertragung möglich sind, werden praktische Systeme durch Störungen des CSI beeinträchtigt, welche z.B. durch verrauschten Pilotsignale, Quantisierungs- und Verzögerungseffekte bei Feedback- und Backhaul-Übertragung verursacht werden. Zwar können Backhaul-Latenzen durch Infrastrukturerneuerungen verringert werden, dafür sind jedoch hohe Investitionen erforderlich.

Diese Arbeit stellt einen alternativen Ansatz vor, welcher die Eigenschaften der Infrastruktur akzeptiert und den Einfluss nicht-perfekter Kanalkennntnis durch robuste Signalverarbeitung mindert. Es wird ein Zweistufenansatz präsentiert, bei dem zunächst die Qualität der Kanalinformation verbessert wird und anschließend robuste Vorverzerrungstechniken eingeführt werden, welche statistische Seiteninformationen über die Kanalunsicherheit ausnutzen. Ein wesentlicher Aspekt dieser Arbeit bezieht sich auf Techniken für verteilte Vorverzerrung, welche gegenüber zentralisierter Verarbeitung deutliche Gewinne aufweist.

# Acknowledgement

This thesis summarizes my work at the Vodafone Chair Mobile Communications Systems at Technische Universität Dresden. In particular, I would like to thank Prof. Gerhard Fettweis for giving me the opportunity to be a part of his versatile research team and for affording me his scientific expertise and guidance during the last few years. He gave me the chance to work in a variety of projects. Beginning with analyzing channel measurements within the renowned EASY-C project (BMBF), I moved on to the DFG focus program COIN, where I worked on cooperative transmission strategies. I participated in the EU project ARTIST4G, which received significant recognition by providing a framework for an effective integration of theoretical multi-cell transmission techniques in practical cellular systems. I also contributed to the Vodafone industry project ACDC, and I am currently working in the ambitious research project iJOIN, which investigates practical realizations of cloud communication systems. Beside numerous valuable contacts, professional and personal experiences, I have had the opportunity to create parts of this work within the scope of these projects.

The final version of this thesis would not have been possible without the support of Dr. Eckhard Ohlmer, Dr. Andreas Festag, Michael Grieger, and Vinay Suryaprakash. Their careful review of the document, their comments, and corrections helped to improve the work significantly. Moreover, I would like to express my gratitude to Prof. Rudolf Mathar for refereeing this thesis and giving my valuable hints for the defense.

Besides the scientific work, I have especially enjoyed the inspirational atmosphere at the Vodafone chair created by the members' richness in personality, talent, and culture. In addition to the already mentioned, I want to exemplarily thank Patrick Grosa, Rohit Datta, Fabian Diehm, Jan Dohl, Najeeb ul Hassan, Walter Nitzold, Ines Riedel, Björn Almeroth, Nicola Michailow, Jens Bartelt, Stefan Wesemann, Lukas Landau, and Tobias Seifert.

Finally, I want to thank my family, all my friends, and especially my girlfriend Deborah who made the time as a PhD student a memorable and exciting period of my life.



# Contents

<b>Abstract</b>	<b>vii</b>
<b>Zusammenfassung</b>	<b>viii</b>
<b>Acknowledgement</b>	<b>ix</b>
<b>List of Figures</b>	<b>xiii</b>
<b>List of Tables</b>	<b>xvii</b>
<b>Abbreviations</b>	<b>xix</b>
<b>Symbols</b>	<b>xxii</b>
<b>1 Introduction</b>	<b>1</b>
1.1 State of the Art . . . . .	2
1.2 Contribution of this Work . . . . .	4
1.3 Outline . . . . .	5
<b>2 Fundamentals</b>	<b>7</b>
2.1 System Setup . . . . .	7
2.1.1 Inter-Cluster Interference . . . . .	9
2.2 Data Transmission . . . . .	11
2.2.1 Achievable Rate . . . . .	12
2.2.2 Imperfect CSI at the Receiver . . . . .	13
2.2.3 Imperfect CSI at the Transmitter . . . . .	14
2.2.4 Rate with Outage . . . . .	15
2.2.5 Basic Precoding Strategies . . . . .	15
2.3 Feedback Signaling . . . . .	19
2.3.1 CSI Feedback Chain . . . . .	19
2.3.2 Simplified CSI Model . . . . .	21
2.3.3 CSI in Distributed Setups . . . . .	22

<b>3</b>	<b>Signaling Optimization</b>	<b>23</b>
3.1	Feedback Signaling . . . . .	23
3.1.1	Where to Predict the Channel in Cooperative Setups? . . . . .	23
3.1.2	Feedback with Outage . . . . .	32
3.1.3	Feedback Strategies in Cooperative Setups . . . . .	41
3.2	Forward Signaling . . . . .	55
3.2.1	Effective Rate Optimization . . . . .	56
3.2.2	Performance Evaluation . . . . .	58
3.3	Summary . . . . .	61
<b>4</b>	<b>Precoder Optimization</b>	<b>63</b>
4.1	Centralized Precoding . . . . .	63
4.1.1	Objective . . . . .	64
4.1.2	Optimization with perfect CSI . . . . .	66
4.1.3	Robust Optimization with imperfect CSI . . . . .	68
4.1.4	Multi-Cell Precoder Optimization based on SOCP . . . . .	70
4.1.5	Performance Evaluation . . . . .	71
4.2	Distributed Precoding . . . . .	75
4.2.1	Objective . . . . .	75
4.2.2	Robust Distributed Optimization . . . . .	76
4.2.3	Performance Evaluation . . . . .	80
4.3	Summary . . . . .	87
<b>5</b>	<b>Conclusions</b>	<b>89</b>
<b>A</b>	<b>Adapted Quantization Model</b>	<b>93</b>
A.1	Independent Input Variables . . . . .	93
A.2	Correlated Input Variables . . . . .	94
<b>B</b>	<b>Where to Predict the Channel over Correlated Sub-Carriers?</b>	<b>97</b>
B.1	CSI Feedback Chain . . . . .	97
B.2	Channel Prediction at the User Equipment . . . . .	98
B.3	Channel Prediction at the Base Station . . . . .	100
B.4	Equivalence of P-UE and P-BS . . . . .	101
B.5	Joint Channel Prediction . . . . .	102
<b>C</b>	<b>Precoding Matrix Optimization</b>	<b>103</b>
C.1	Relation between MSE and Achievable Rate . . . . .	103
C.2	Weighted Sum MSE Minimization with Perfect CSI . . . . .	104
C.3	Weighted Sum MSE Minimization with Imperfect CSI . . . . .	106
C.4	Local Weighted Sum MSE Minimization with Remote Precoding Matrices . . . . .	108

Contents	xiii
<b>Bibliography</b>	<b>110</b>
<b>List of Publications</b>	<b>119</b>
<b>Curriculum Vitae</b>	<b>123</b>



# List of Figures

2.1	Basic cellular system setup for cooperative multi-cell transmission in the downlink and CSI feedback in the uplink. . . . .	8
2.2	1-dimensional setup of BSs, UEs in combination with their distances. . . . .	9
2.3	SINR over the SNR received at the cell edge, for a $K = M = 2$ setup and different numbers of outer-cluster BSs. . . . .	10
2.4	Ergodic achievable rate performance as a function of the cell edge SNR for four basic precoding algorithms under perfect CSI conditions. . . . .	16
2.5	Ergodic achievable rate performance including inter-cluster interference under perfect CSI conditions. . . . .	17
2.6	Ergodic achievable rate performance including inter-cluster interference under imperfect CSI conditions. . . . .	18
2.7	Feedback model for reporting CSI back to the transmitter side. . . . .	20
3.1	Feedback of UE $k \in \mathcal{K}_m$ for DP, where less outdated CSI is available at the local BS $m$ and more outdated CSI arrives at the remote BS $\bar{m}$ . . . . .	24
3.2	CSI feedback chain, where channel prediction is performed at the UE (P-UE)	26
3.3	CSI feedback chain, where channel prediction is performed at the BS (P-BS)	27
3.4	Average channel uncertainty for different prediction options. . . . .	31
3.5	Illustration of potentially available channel observations, where the gray slots are available with a certain probability, while the black slot are not considered for processing. . . . .	33
3.6	Relation between outage probability, channel uncertainty and the number of signaling resources for uplink feedback transmission. . . . .	39
3.7	Optimized signaling amount based on the number of uplink signaling resources $N_S$ . . . . .	39
3.8	Channel uncertainty for optimized signaling over uplink signaling resources for $W = 10$ and $\Delta = 5$ ms. . . . .	40
3.9	Channel uncertainty for optimized signaling over uplink feedback resources for $W = 5$ and $\Delta = 10$ ms. . . . .	41

3.10	Impact of different parameters on the CSI quality in cooperative setups for downlink channel observation and uplink feedback transmission. . . . .	42
3.11	Cooperatively decoded feedback . . . . .	43
3.12	Degree of cooperation for different feedback strategies, where c) and d) do only apply for DP . . . . .	44
3.13	Degree of knowledge at the BSs and the CN about channel observations, which have been fed back from the UE . . . . .	45
3.14	Relation between channel uncertainty, outage probability and number of signaling resources for $\delta = 0.5$ . . . . .	51
3.15	Relation between reliability and accuracy of uplink CSI feedback . . . . .	51
3.16	Relation between channel uncertainty, outage probability and number of signaling resources for $\delta = 0.3$ . . . . .	52
3.17	Relation between reliability and accuracy of uplink CSI feedback for different evaluation metrics . . . . .	53
3.18	Achievable rate for downlink transmission comparing CP and DP . . . . .	54
3.19	Achievable rate for downlink transmission comparing different optimization metrics . . . . .	54
3.20	Resource segmentation with payload data, pilots and precoded pilots . . . . .	55
3.21	Signaling chain for precoded pilots. . . . .	57
3.22	Effective rate optimization . . . . .	59
3.23	Effective rate with different block sizes . . . . .	59
4.1	Achievable rate for centralized precoding without inter-cluster interference. . . . .	72
4.2	Ratio between smaller transmit power and full transmit power. . . . .	73
4.3	Achievable rate for centralized precoding with inter-cluster interference. . . . .	74
4.4	Degree of knowledge at each BS with fully shared (FS) feedback . . . . .	77
4.5	Achievable rate for distributed precoding with centralized algorithms . . . . .	81
4.6	Achievable rate for distributed precoding without inter-cluster interference . . . . .	82
4.7	Difference between the maximum and minimum transmit power . . . . .	83
4.8	Achievable rate for distributed precoding with inter-cluster interference . . . . .	83
4.9	Achievable rate for distributed precoding considering outages for feedback transmission with user separation $\delta = 0.5$ . . . . .	84
4.10	Achievable rate for distributed precoding considering outages for feedback transmission with user separation $\delta = 0.4$ . . . . .	85

---

4.11	Achievable rate for distributed precoding considering fully shared feedback	86
B.1	Feedback model for reporting CSI back to the BS. . . . .	98
B.2	Channel feedback chain with prediction at the UE (P-UE) . . . . .	99
B.3	Channel feedback chain with prediction at the BS (P-BS) . . . . .	100



# List of Tables

3.1	Wirtinger derivatives of a vector . . . . .	28
4.1	Wirtinger derivatives of a matrix . . . . .	66
4.2	Simulation Parameters . . . . .	72



# Abbreviations

3GPP	third generation partnership project
AWGN	additive white Gaussian noise
bpcu	bit per channel use
BS	base station
CEW	channel dependent error weighting
CN	central node
CoMP	coordinated multi-point
CP	centralized precoding
CSI	channel state information
CSK	central statistical knowledge
CSIR	CSI at the receiver
CSIT	CSI at the transmitter
dB	decibel
DP	distributed precoding
FDD	frequency division duplex
FS	fully shared (feedback)
H-ARQ	hybrid automatic repeat request
IEEE	institute of electrical and electronics engineers
i.i.d.	independent and identically distributed
ISD	inter-site distance
KKT	Karush Kuhn Tucker (conditions)
LSK	local statistical knowledge
LTE	long term evolution
MIMO	multiple-input multiple-output
ML	maximum likelihood
MMSE	minimum mean square error
MSE	mean square error
MSK	mean statistical knowledge
MU-MIMO	multituser-MIMO
NS	not shared (feedback)
N-WF	normalized zero-forcing
N-ZF	normalized Wiener filter
OFDM	orthogonal frequency division multiplexing

---

P-BS	prediction at the BS
P-UE	prediction at the UE
PU	processing unit
PS	partially shared (feedback)
QoS	quality of service
O-ZF	optimal zero-forcing
SIC	successive interference cancellation
SINR	signal-to-interference-and-noise ratio
SIR	signal-to-interference ratio
SISO	single-input single-output
SNR	signal-to-noise ratio
SOCP	second order cone program
RS	remotely shared (feedback)
UE	user equipment
UEW	uniform error weighting
WF	Wiener filter
WSMSE	weighted sum MSE
WSR	weighted sum rate
ZF	zero forcing

# Symbols

## Notation

- ▷  $\mathbf{A} \in \mathbb{C}^{m \times n}$  : Uppercase boldface letters denote matrices of dimension  $m \times n$  with elements of the set  $\mathbb{C}$  and likewise for the real set.
- ▷  $\mathbf{a} \in \mathbb{C}^{m \times 1}$  : Lowercase boldface letters denote column vectors of dimension  $m \times 1$  with elements of the set  $\mathbb{C}$  and likewise for the real set.
- ▷  $a, A$  : Normal letters denote scalar values.
- ▷  $[\mathbf{A}]_{i,j}$  : Denote the entry in the  $i$ -th row and the  $j$ -th column.
- ▷  $[\mathbf{a}]_i$  and  $a_i$  : Both notations are exchangeably used to denote  $i$ -th entry of vector  $\mathbf{a}$
- ▷ Random variables and their respective realization will not be distinguished for the brevity of notation. The notation  $p(x = x')$  or  $\Pr(x \leq x')$  is used to indicate a particular realization  $x'$  of random variable  $x$
- ▷ Indices of variables are denoted by italic letters, e.g.,  $\mathbf{a}_b$  refers to a vector of BS  $b$ .
- ▷ Labels to distinguish different variables are denoted by non-italic letters, e.g.,  $\mathbf{a}_b$  refers to a vector w.r.t. the BS side

## Symbols

$\mathbf{A}$	diagonal scaling matrix for calibrating the adapted quantizer model
$\mathbf{B}, \mathbf{B}_m, \bar{\mathbf{B}}_k$	precoding matrix, precoding matrix at BS $m$ , precoding matrix for UE $k$
$\tilde{\mathbf{B}}$	non scaled precoding matrix
$\mathbf{C}, \mathbf{C}_q, \mathbf{C}_t$	covariance matrix of the channel, the quantization noise, the precoded channel
$\mathbf{d}, \mathbf{d}_k$	data symbol vector, data symbol vector of UE $k$
$\mathbf{D}$	regularization matrix applied for robust precoding
$\mathbf{E}, \mathbf{E}_k, \mathbf{E}_{k,m}$	error matrix, error matrix to UE $k$ , error matrix between BS $m$ and UE $k$
$\hat{\mathbf{E}}_{k,m}, \tilde{\mathbf{E}}_{k,m}$	channel uncertainty matrix of the simplified CSI model between BS $m$ and UE $k$ , channel uncertainty matrix of the simplified CSI model between BS $m$ and UE $k$ common at all BSs

$\mathbf{g}, \mathbf{G}, \mathbf{G}_P$	channel prediction vector, channel prediction matrix, filter matrix for estimating precoded pilots
$\mathbf{H}, \mathbf{H}_k, \mathbf{H}_{k,m}$	MIMO channel matrix, MIMO channel matrix to UE $k$ , MIMO channel matrix between BS $m$ and UE $k$
$\hat{\mathbf{H}}, \hat{\mathbf{H}}_k, \hat{\mathbf{H}}_{k,m}$	estimate of the MIMO channel matrix, estimate of MIMO channel matrix to UE $k$ , estimate of MIMO channel matrix between BS $m$ and UE $k$
$\mathbf{M}, \mathbf{M}^{\text{MMSE}}$	MSE matrix, MMSE matrix
$\mathbf{n}, \mathbf{n}_k$	AWGN at all receivers, AWGN at receiver $k$
$\mathbf{P}$	diagonal scaling matrix multiplied with the non scaled precoding matrix
$\mathbf{P}_{\text{out}}$	diagonal matrix with $W_{\text{max}}$ outage probabilities on the diagonal
$\mathbf{q}$	quantization noise of subsequent channel coefficients
$\mathbf{S}, \mathbf{S}_i$	random outage matrix, realization $i$ of outage constellation
$\mathbf{T}_k$	precoded channel observed at UE $k$
$\mathbf{T}_{k,l}$	precoded channel between data intended for UE $l$ observed at UE $k$
$\mathbf{U}, \mathbf{U}_k$	receive filter, receive filter of UE $k$
$\mathbf{W}, \mathbf{W}_k$	wighting matrix, weighting matrix of UE $k$
$\mathbf{z}$	effective complex additive white Gaussian receiver noise vector for pilot reception
$a$	scaling of the quantizer input to calibrate the adapted quantization model
$b$	scaling of precoding matrix to satisfy the transmit power constraint(s)
$d_{k,m}, d_I$	distance between BS $m$ and UE $k$ , ISD
$R_k, \bar{R}_k, \bar{R}$	achievable rate of UE $k$ , ergodic achievable rate of UE $k$ , average ergodic achievable rate
$\hat{R}_k$	assigned rate of UE $k$
$\bar{R}_{\text{out},k}, \bar{R}_{\text{out}}$	rate with outage of UE $k$ , average rate with outage
$R_S$	uplink signaling rate
$T_C$	coherence time in ms
$\alpha$	path loss exponent
$\beta$	parameter to adjust the mean channel gain
$\gamma$	SNR received at the cell edge without any interference
$\delta$	distance between BS and UE relative to the ISD
$\epsilon_{k,m}$	MSE between the actual channel and the CSI for the link between BS $m$ and UE $k$
$\eta$	isolation of the cluster (gain of outer cluster interference)
$\lambda, \lambda_{k,m}$	mean channel gain, mean channel gain between BS $m$ and UE $k$
$\rho, \rho_m$	transmit power for data and pilots, transmit power restriction at BS $m$
$\varrho_P$	pilot density including pilots from all BS antennas

$\sigma_{I,k}^2$	power of outer cluster interference received at UE $k$
$\sigma_n^2$	power of the receiver noise without any interference
$\sigma_n^2$	power of the receiver noise including potential interference from outer cluster BSs
$\psi_k$	back-off factor for optimizing the rate with outage
$M, M_{OC}$	number of BSs within the considered cluster, number of BS outside the considered cluster
$K$	number of UEs
$B, B_m$	number of overall BS antennas, number of antennas at BS $m$
$U, U_k$	number of overall UE antennas, number of antennas at UE $k$
$L, L_t, L_f$	number of transmit symbols within a transmission block, within a transmission block in time direction, within a transmission block in frequency direction
$N_P, N_{PS}$	number of pilot signals, number of precoded pilot signals per transmission block, respectively
$N_S$	number of uplink signaling resources
$Q$	number of quantization bits
$W, W_{\max}$	number of samples used for processing, number of samples considered for processing
$\Delta_F, \Delta_B$	number of delayed transmission blocks for feedback transmission, for backhaul transmission, respectively
$\mathbb{R}$	set of real numbers
$\mathbb{C}$	set of complex numbers
$\emptyset$	empty set
$\mathcal{M}$	set of BSs
$\mathcal{K}, \mathcal{K}_m$	set of UEs, set of UEs assigned to BS $m$
$\mathcal{S}$	set of outage constellations
$(\cdot)^*$	complex conjugate
$(\cdot)^{-1}$	inverse matrix
$(\cdot)^T$	transpose matrix
$(\cdot)^H$	complex conjugate transpose matrix
$\mathbf{I}_N$	identity matrix of dimension $N \times N$
$\sigma_a$	standard deviation of random variable $a$
$\mu_a$	mean of random variable $a$

## Functions

$\otimes$	Kronecker product
$\text{var}(\cdot)$	variance
$\mathbb{P}\{\cdot\}$	probability

---

$\mathbb{E}_{\mathbf{a}} \{f(\mathbf{a})\}$	expectation of a function $f(\mathbf{a})$ with respect to the distribution of the random vector $\mathbf{a}$
$\mathbb{E}_{\mathbf{a} \mathbf{b}} \{f(\mathbf{a})\}$	conditional expectation of a function $f(\mathbf{a})$ with respect to the distribution of the random vector $\mathbf{a}$ , conditioned on $\mathbf{b}$
$ \cdot $	absolute value of a number or cardinality of a set as will be clear from the context
$\ \cdot\ _2$	vector-2-norm
$\ \cdot\ _F$	Frobenius matrix norm
$\text{tr}(\cdot)$	matrix trace
$\det(\cdot)$	matrix determinant
$\text{diag}(\mathbf{a})$	creates a square diagonal matrix from vector $\mathbf{a}$
$\text{diag}^{-1}(\mathbf{A})$	returns the main diagonal of square matrix $\mathbf{A}$
$\text{dg}(\mathbf{A})$	replaces each off diagonal element with zero
$\text{blkdiag}(\mathbf{A}_1, \dots, \mathbf{A}_M)$	creates a block diagonal matrix out of the matrices $\mathbf{A}_1, \dots, \mathbf{A}_M$
$\text{vec}(\mathbf{A})$	stacks the columns of matrix $\mathbf{A}$ into a column vector denoted by $\vec{\mathbf{A}}$
$\text{shr}(\mathbf{A})$	shrinks matrix $\mathbf{A}$ by canceling all rows and columns which have only zero elements
$\text{shr}(\mathbf{A}, N)$	as $\text{shr}(\mathbf{A})$ , but with additional shrinking of $\mathbf{A}$ to an $N \times N$ matrix by canceling columns at the right and rows at the bottom.
$\mathcal{N}(\boldsymbol{\mu}, \mathbf{C})$	(multi-variate) Gaussian distribution
$\mathcal{N}_{\mathbb{C}}(\boldsymbol{\mu}, \mathbf{C})$	complex (multi-variate) Gaussian distribution
$\max_a f(a)$	returns the maximum of function $f(a)$ with respect to its argument $a$
$\arg \max_a f(a)$	returns the argument which maximizes the function $f(a)$

# Chapter 1

## Introduction

Mobile communications have boosted economic growth and improved the quality of education and health care all over the world during the last few decades [Int07]. Mobile devices have especially benefited from Moore's Law, which states that the transistor density on integrated circuits doubles approximately every 18 months [Moo65]. A constant increase in processing power and memory size has enabled rich media applications to run on smart phones, tablets, and laptops. Particularly, mobile video streaming and social networking services have gained significant traction and have led to a constant growth in mobile data traffic, which is expected to reach a 13-fold increase between 2012 and 2017 [Cis13]. Since smart phones are expected to generate two thirds of the mobile traffic in 2017, the demand for increasing capacities of cellular systems is of significant importance.

In order to support data intensive mobile services, network operators are requested to provide higher throughput per area. This goal can be achieved by three basic strategies: additional bandwidth, base station (BS) densification, and an increase in spectral efficiency [Nok12]. The first two approaches are typically linked to large investments, which is not necessarily the case for deriving substantial spectral efficiency gains. For this purpose, a prominent method is to exploit the spatial dimension by employing multiple antennas at the transmitter and the receiver side, and transferring multiple data streams in parallel [FG98, Tel99]. Multi antenna systems, also referred to as multiple-input-multiple-output (MIMO) are already being used in current communication standards such as 3rd Generation Partnership Project Long Term Evolution (3GPP-LTE) Advanced [3GP13] and IEEE (Institute of Electrical and Electronics Engineers) 802.11n [IEE09].

In MIMO systems, the number of parallel data streams is restricted to the minimum between the number of transmit and receive antennas. In cellular systems, the BS side typically allows a much larger number of antennas to be employed, when compared to the user equipment (UE) side. In order to preserve the full multiplexing gain, multiple users can be combined to obtain a larger, only partially connected antenna array and building a multiuser-MIMO (MU-MIMO) system [GKH<sup>+</sup>07]. Since users are not able to directly exchange messages inter-user interference needs to be handled at the BS side [CS03]. In

this regard, downlink transmission is particularly challenging, since spatial pre-processing filters (also referred to as precoding) of multiple users are coupled and need to be optimized jointly before the actual transmission takes place [WES06, SVH06]. Instead of installing large antenna arrays at each BS, similar effects can be achieved by utilizing existing antennas at multiple BSs, and combining them into a virtual antenna array distributed over a larger area, while the required information is exchanged between BSs via backhaul connections [ZD04, KFV06]. Such a cooperative MU-MIMO system is also referred to as network MIMO. Precoding for cooperative multi-cell transmission is characterized by its transmit power constraints per group of antennas [Yu06], which result in more challenging optimization problems compared to single-cell transmission with a sum power constraint [KSKS12].

Shaping interference between users w.r.t. the current channel situation requires channel state information (CSI) to be available at the BS side. In frequency division duplex (FDD) systems, CSI can be obtained by observing the channel in the downlink and feeding the information back to the BSs. In the presence of delays between channel observation and actual data transmission along with time variations of the mobile channel due to user mobility, CSI becomes outdated, and inaccurate precoding can cause substantial performance losses [Jin05].

In the context of imperfect CSI, backhaul latency has a major impact on practical systems, which typically results from routing over multiple network nodes in combination with protocol stack delays. Typical backhaul latencies are in the range of a pedestrian user's coherence time. In order to retain the opportunity to serve these users cooperatively, advanced robust interference mitigation schemes can provide data rate gains by incorporating statistical knowledge of the channel state uncertainty, instead of treating the available information as being perfect [Die08].

## 1.1 State of the Art

Early works in the area of precoding for MU-MIMO downlink systems (also known as MIMO broadcast channel) focused on linear techniques like zero-forcing (ZF) and Wiener filtering (WF) [JKG<sup>+</sup>02, DHJU03a]. Although achieving capacity requires non-linear dirty paper coding [Cos83, CS03], practical schemes suffer from high complexity [PHS05, HPS05, KJUB05, HIRF05], which is critical due to the delay sensitive nature of the broadcast channel. For this reason, this work focuses on more practical linear precoding strategies. For optimizing the precoding filter, several works consider target metrics such as mean square error (MSE) [HUSJ06, SSB07], signal-to-interference-and-noise-ratio (SINR) [YL07], or transmission rate employing linear [SSB08] or optimal receivers [SVH06, CACC08]. The latter case provides larger rate performance and is of main relevance for this thesis. Besides different objectives like fairness in terms of balancing user performance [TCJ07, MF008, TUNB09] under transmit power constraints, or

power minimization with quality of service (QoS) requirements [SB04, LSK06, WES06], this work focuses on performance maximization under transmit power constraints. This is motivated by passing fairness aspects to the scheduling scheme, which allocates resources to particular user groups [YG06, TCRY08]. However, fairness within such a group can be affected by user weights, which are taken into account by the precoding scheme [CACC08].

Due to the high potential gains of cooperative multi-cell transmission [Wil83, SZ01, ZD04, KfV06], precoding schemes have been adapted by incorporating more challenging transmit power constraints per BS [SSVB08, Zha10, KSKS12]. For the schemes previously mentioned, it's assumed that perfect CSI is available at the BS side. However, such idealistic situation is barely the case in practical systems. Precoding strategies which are robust against imperfect CSI have been presented for single-cell setups [DHJU03b, SD06, CJCU08]. Robust MSE optimal precoding for multi-cell systems has been addressed in [VBS09] for bounded channel uncertainty, while the schemes in [BCV11, BV12] consider unbounded CSI imperfections. The scheme in [LBS12] tries to maximize data rate based on particle swarm optimization.

While the aforementioned multi-cell precoding schemes account for centralized processing, distributed strategies with different CSI versions at the cooperating BSs have been addressed in [ZG10] for a two-cell two-user setup, where a hierarchical codebook with poor backhaul capacity was assumed. The authors stated that it is beneficial to reduce local CSI accuracy in order to achieve consistent knowledge, if the precoding scheme is not aware of inconsistencies. Limiting the amount of backhaul exchange for cooperative precoding was also studied in [MF07, NEHA08, SSPS09]. The achievable rate region for the case of distributed BS cooperation with full data sharing while using only local CSI is presented in [BZGO10]. The authors proposed a virtual SINR framework for distributed beamforming design based on uplink-downlink duality theory [SB04]. A degrees of freedom analysis along with a two-user distributed precoding (DP) scheme was presented in [dKG12].

In addition to designing the precoding filters in order to be robust against CSI imperfections, this thesis studies strategies for increasing the actual accuracy of CSI, which leads to additional robustness of the data transmission. In this regard, [CJCU07] emphasized the effects of noisy pilot reception, CSI quantization and feedback delays in single-cell MU-MIMO systems. Among other things the authors employed a minimum MSE (MMSE) channel prediction filter at the UE side. The impact of channel prediction in coordinated multi-point (CoMP) setups have been evaluated based on measurements in [LPA<sup>+</sup>12]. An overview of feedback quantization strategies in FDD systems is given in [LHL<sup>+</sup>08].

Models which abstract the effects of quantization based on rate distortion theory are used in [MRF10, MF11]. Aspects of how to feed CSI back in cooperative systems have been addressed in [PHG09], introducing a framework which accounts for feedback errors due to imperfect uplink transmission. The authors compared direct decoding of feedback at all cooperating BSs with the case where only the local BS decodes CSI and forwards it to

the other BSs via a limited rate backhaul. Apart from that, the relation between feedback resolution and how frequently it is transmitted is analyzed in [KLC11].

## 1.2 Contribution of this Work

This thesis contributes to the area of signaling optimization as well as the field of precoding under imperfect CSI conditions. Signaling for DP under a latency affected backhaul with channel prediction and quantized feedback was investigated in [FOF13b]. Contrary to the assumptions in [CJCU07, MRF10], it was found that placing the predictor at the BS side is preferable to predicting at the UE side. The latter one suffers from determining the prediction horizon, while multiple delays occur in the system. While the derivations in [FOF13b] are restricted to the case of independent sub-carriers, the results could be extended to a more general case of correlated sub-carriers in [FOF13a].

In [FF11], the distribution of CSI for different feedback strategies has been derived. It has been stated that possible outages for CSI feedback in the uplink result in a Gaussian mixture distribution. Similar to [PHG09], multi-cell feedback via uplink decoding at all BSs have been compared with just local decoding and forwarding via backhaul connections. In contrast to [PHG09], the framework in [FF11] assumes backhaul delays which are of major practical interest. It could be shown that the optimal feedback strategy depends on the user location within the cooperation area. Additionally, a combined strategy has been investigated where the BS exploits both, CSI from uplink feedback, as well as delayed CSI from backhaul forwarding.

Apart from uplink feedback, forward signaling in the downlink is required to make the precoded channel available to the UEs, in order to allow coherent detection of the precoded data. In this regard, analog and digital forwarding strategies have been investigated in [FSF13]. It could be shown that analog signaling outperforms digital strategies as soon as CSI at the transmitter side (CSIT) is only imperfectly available. A further result is that the impact of impaired precoded CSI at the receiver (CSIR) is of little relevance when compared to CSIT imperfections.

Robust MMSE precoding for cooperative multi-cell transmission has been presented in [FF12], considering four different MSE related objectives. Compared to [VBS09], the channel uncertainty is unbounded as is typically the case in practical systems. The work is based on a non-robust optimization framework presented in [SSVB08], where the original problem is transferred into a second order cone program (SOCP), which can be solved by standard optimization software.

Furthermore, the sum rate optimal precoding strategies of [CACC08, KSKS12] could be extended to solutions which are robust against CSI imperfections [FF13b]. The schemes exploit a basic relation between achievable rate and MSE. In contrast to [NGS12], which follows a similar approach and presents a robust solution for interference alignment, the

algorithm in [FF13b] can be applied for cooperative precoding with full data sharing. While [FF12, FF13b] focus on centralized precoding (CP), a novel solution for distributed robust precoding has been presented in [FF13a]. The scheme provides the ability to exploit more accurate CSI of local users and is aware of inconsistent channel knowledge.

## 1.3 Outline

The rest of this thesis is organized as follows:

- ▷ **Chapter 2:** introduces the system setup and main assumptions required for further derivations
- ▷ **Chapter 3:** focuses on aspects of signaling optimization in cooperative scenarios in order to provide CSIT as well as precoded CSIR
- ▷ **Chapter 4:** presents robust solutions for precoding under imperfect CSI conditions. In this section CP as well as DP schemes are presented
- ▷ **Chapter 5:** summarizes the contributions of this thesis and gives an outlook to open problems and future topics of interest



# Chapter 2

## Fundamentals

This chapter first introduces the basic cooperative cellular system setup as well as the entities involved in Section 2.1. Functionalities and major assumptions are explained and motivated. Furthermore, the concept of CP and DP is explained and an inter-cluster interference model is presented. Section 2.2 introduces downlink data transmission with cooperative multi-cell precoding based on CSI. Imperfect channel knowledge is addressed looking at both, the transmitter and the receiver side. Uplink feedback signaling is explained in Section 2.3.

### 2.1 System Setup

The network MIMO system considered in this work is illustrated in Fig. 2.1. It consists of  $M$  cooperating BSs and  $K$  UEs, where  $\mathcal{M} = \{1, \dots, M\}$  and  $\mathcal{K} = \{1, \dots, K\}$  denote the set of BSs and UEs, respectively. The set  $\mathcal{M}$  of cooperating BSs is called cooperation cluster. All  $M$  BSs are connected to a central node (CN), resulting in a star topology (see Fig. 2.1). Of course, practical topologies can have direct connections among BSs. However, all aspects relevant for this work can be inherently addressed by means of the star topology by allowing different qualities of BS-CN connections.

Each UE  $k$  is assigned to a single BS which is referred to as *local* BS.  $\mathcal{K}_m$  denotes the set of UEs which are assigned to BS  $m$ , where  $\cap_{m=1}^M \mathcal{K}_m = \emptyset$  and  $\cup_{m=1}^M \mathcal{K}_m = \mathcal{K}$  need to be satisfied. Every other BS  $l \neq m$  to which UE  $k \notin \mathcal{K}_l$  is not assigned, is called *remote* BS. Considering cooperative transmission, the all BSs in  $\mathcal{M}$  are occasionally referred to as *servicing* BSs in order to distinguish them from BSs outside the cooperation cluster (denoted as *outer-cluster* BSs). In this work, each UE  $k$  is assigned to the BS with the strongest mean channel gain

$$\lambda_{k,m} = \beta d_{k,m}^{-\alpha} \quad (2.1)$$

with path loss exponent  $\alpha$ , distance  $d_{k,m}$  between UE  $k$  and BS  $m$  and coefficient  $\beta$  to further adjust the model, to account for, e.g., shadow fading effects [Tec10]. The mean

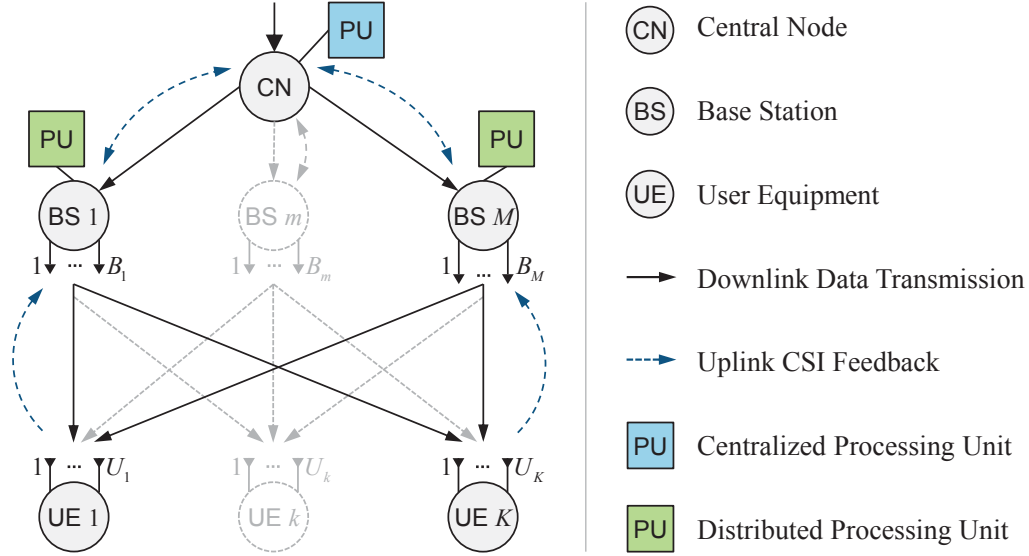


**Fig. 2.1:** Basic cellular system setup for cooperative multi-cell transmission in the downlink and CSI feedback in the uplink.

channel gains of all BS-UE links are collected in matrix  $\Lambda = [\lambda_1, \dots, \lambda_M]$  with  $\lambda_m = [\lambda_{1,m}, \dots, \lambda_{K,m}]^T$ . The set of UEs assigned to BS  $m^*$  results in

$$\mathcal{K}_{m^*} = \left\{ k \in \mathcal{K} \mid m^* = \arg \max_{\forall m} \lambda_{k,m} \right\}. \quad (2.2)$$

Furthermore, each BS  $m$  is equipped with  $B_m$  transmit antennas while each UE  $k$  employs  $U_k$  receive antennas. The overall number of antennas at the BS and UE side is  $B$  and  $U$ , respectively.

This work focuses only on downlink transmission, where CSI is required for precoding the user data. In FDD systems, the downlink channel cannot be observed from uplink pilot signals. Therefore, the downlink channel is observed by the UEs, which feed their knowledge back to the BS side using uplink signaling. Unless stated otherwise, it is assumed that the feedback of each UE  $k$  is decoded only at its local BS  $m$  with  $k \in \mathcal{K}_m$ .

As can be seen in Fig. 2.1, the CN as well as each BS is equipped with a processing unit (PU), used for precoding user data based on CSI feedback. CP refers to the case where each BS forwards the CSI of all its assigned UEs to the CN. The PU computes the precoding matrix based on the available CSI, precodes the user data and forwards the results to the respective BS, from where it is transmitted. In contrast, for DP, each BS forwards its CSI to all other BSs within the cooperation cluster. Assuming the star topology, all CSI is routed via the CN. At the end, each BS has a version of the complete network MIMO channel available locally. However, due to backhaul constraints, such as latency, CSI from other BSs can have different accuracies, while CSI from the assigned UEs is locally available and not affected by backhaul impairments at all. This implies that each BS has a different CSI version available. Based on its *local* CSI, each distributed BS

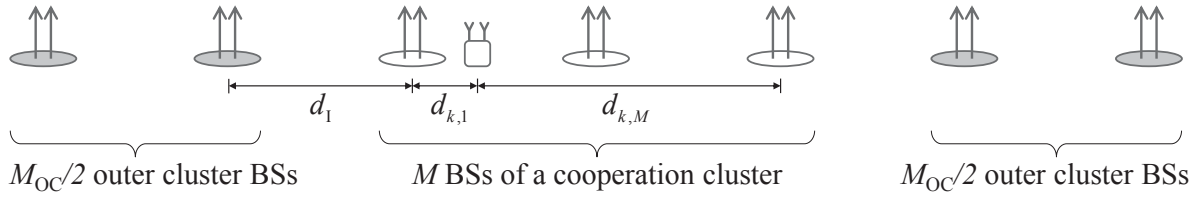


**Fig. 2.2:** 1-dimensional setup of BSs, UEs in combination with their distances.

performs the computation of the precoding matrix individually. The CN forwards the data of all users to all BSs. Each BS filters the data with its locally computed precoding matrix and transmits the results. Note that precoding with different CSI versions at the BSs can lead to substantial performance losses due to inconsistencies. On the other hand, the CSI quality of local UEs is improved.

### 2.1.1 Inter-Cluster Interference

In addition to the  $M$  BSs within a cooperation cluster,  $M_{OC}$  BSs outside the cluster transmit data to their own UEs and cause inter-cluster interference for all other UEs, as illustrated in Fig. 2.2. Among others, the interference a UE receives from outer-cluster BSs depends on their scheduling decision and precoding. However, this work abstracts from these issues by assuming outer-cluster BSs transmit with constant power  $\rho$  equally in all directions and on all resources, which is a realistic assumption when no interference coordination is performed between cooperating clusters. Furthermore, the interference each UE  $k$  receives from outer-cluster BSs is assumed to be complex Gaussian distributed with zero mean and variance  $\sigma_{I,k}^2$ . For the 1-dimensional model, where all BSs are located on a line (see Fig. 2.2), the interference variance results in

$$\sigma_{I,k}^2 = \eta\rho\beta \sum_{i=1}^{M_{OC}/2} [(id_1 + d_{k,1})^{-\alpha} + (id_1 + d_{k,M})^{-\alpha}], \quad (2.3)$$

where the first and the second part of (2.3) refers to the  $M_{OC}/2$  outer cluster BSs on the left and on the right hand side of the considered cluster, respectively (see Fig. 2.2). Parameter  $\eta$  is introduced for describing the isolation of a cluster, motivated by antenna tilting in real 3-dimensional setups or methods such as the *tortoise concept*, where outer cluster radiation is reduced [MZ11] and overlapping clusters are introduced for serving all areas cooperatively. Note that this thesis does not intend to emphasize outer-cluster interference as accurately as possible, but provides the opportunity to evaluate the results presented for different levels of cluster isolation.

In order to analyze the interference limited behavior of cellular systems, the SINR observed at each UE  $k$  is defined as the ratio of the potentially useful received signal power and the sum of receiver noise  $\sigma_n^2$  and outer-cluster interference  $\sigma_{I,k}^2$  received at UE  $k$ . Its logarithmic

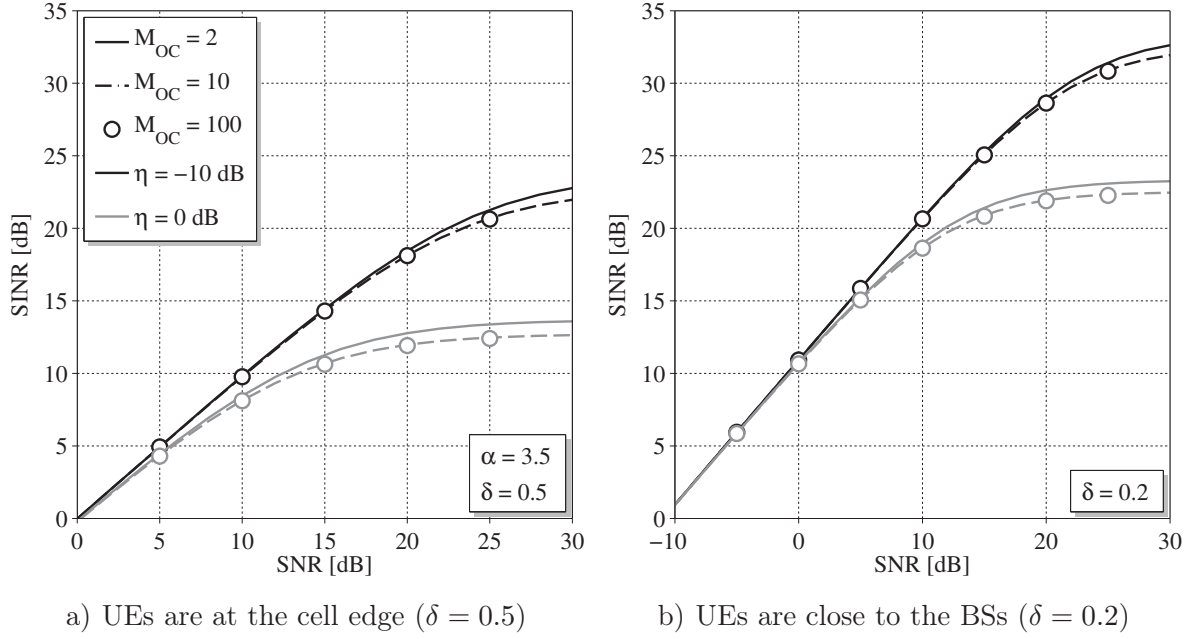


**Fig. 2.3:** SINR over the SNR received at the cell edge, for a  $K = M = 2$  setup and different numbers of outer-cluster BSs.

representation reads

$$\text{SINR}_k = 10 \log_{10} \left( (\sigma_n^2 + \sigma_{1,k}^2)^{-1} \frac{\rho \beta}{K} \sum_{m=1}^M d_{k,m}^{-\alpha} \right), \quad \forall k. \quad (2.4)$$

The transmit power  $\rho$  has an impact on both, the useful signal received from the serving BSs as well as the interference from the outer-cluster BSs. Note that (2.4) is based on the idealistic assumption that each BS  $m$  transmits  $1/K$ -th of its power to each user and completely cancels out inter-user interference.

In the following, a simple setup with  $K = 2$  UEs and  $M = 2$  cooperating BSs as well as a variable number of outer-cluster BSs  $M_{OC}$  is considered. It is assumed that both UEs are located symmetrically between the two serving BSs (i.e.,  $d_{1,1} = d_{2,2}$  and  $d_{1,2} = d_{2,1}$ ). Defining the relative distance  $\delta = d_{k,m}/d_1$ ,  $\forall k \in \mathcal{K}_m$  as the ratio between actual distance and inter-site distance (ISD), the SINR for each UE  $k$  results in

$$\text{SINR} = 10 \log_{10} \left( \frac{\delta^{-\alpha} + (1 - \delta)^{-\alpha}}{\gamma^{-1} 2^{\alpha+1} + 2\eta \sum_{n=1}^{M_{OC}/2} (n + \delta)^{-\alpha} + (n + 1 - \delta)^{-\alpha}} \right). \quad (2.5)$$

The cell edge signal-to-noise-ratio (SNR) is defined as the ratio of the signal power from the local BS received at the cell edge and the power of the receiver noise  $\sigma_n^2$ . It reads

$$\gamma = \beta \left( \frac{d_1}{2} \right)^{-\alpha} \cdot \frac{\rho}{\sigma_n^2}, \quad (2.6)$$

while its logarithmic representation in decibel (dB) is  $\text{SNR} = 10 \log_{10}(\gamma)$ .

In this work, the cell edge SNR often acts as abscissa, since it corresponds to adjusting the transmit power  $\rho$ , which is of interest from a mobile operators point of view.

Fig. 2.3 shows the SINR observed at a UE as a function of the cell edge SNR (the logarithmic version of the definition in (2.6)) for different numbers of outer-cluster BSs  $M_{\text{OC}}$ . According to the urban macro-cell scenario specified in [Tec10], the path loss exponent is chosen to be  $\alpha = 3.5$ . In the left plot, the UEs are located at the cell edge between the two cooperating BSs. For the low SNR regime (below 5 dB), inter-cluster interference has little impact and the SINR is close to the SNR. For moderate SNRs (5 - 20 dB), interference gains influence, while in the high SNR region (more than 20 dB) the SINR saturates and the quality of the received signal cannot be further improved by increasing the transmit power. In the low noise region, the SINR is improved by scaling the outer-cluster radiation by  $\eta = -10$  dB.

A similar behavior is shown in Fig. 2.3 b), where the UEs are close to their local BSs ( $\delta = 0.2$ ). Consequently, the received SINR is about 10 dB higher than for users at the cell edge. However, the saturation behavior is very similar in both cases. Additionally, taking  $M_{\text{OC}} = 10$  outer-cluster BSs into account, is sufficient to model outer-cluster interference adequately in both cases, and is used for further evaluations in this work.

## 2.2 Data Transmission

For downlink data transmission, a block fading radio channel, which remains in a constant channel state for the duration of a transmission block is assumed. Such a block consists of  $L = L_t L_f$  channel uses in total, where  $L_t$  and  $L_f$  correspond to channel uses in time and frequency, respectively. The channel of subsequent transmission blocks in time and frequency is basically correlated, as described in more detail in Section 2.3. The data symbols transmitted to all  $K$  UEs within a single channel use, are collected in a vector  $\mathbf{d} = [\mathbf{d}_1^T, \dots, \mathbf{d}_K^T]^T$ . All elements of  $\mathbf{d}$  are assumed to be independent and identically distributed (i.i.d.) with zero mean and unit variance according to  $\mathbf{d} \sim \mathcal{N}_{\mathbb{C}}(\mathbf{0}, \mathbf{I})$ . The data vector is jointly pre-processed by multiplying it with the precoding matrix

$$\mathbf{B} = [\mathbf{B}_1^T, \dots, \mathbf{B}_M^T]^T = [\bar{\mathbf{B}}_1, \dots, \bar{\mathbf{B}}_K], \quad (2.7)$$

where each sub-matrix  $\mathbf{B}_m \in \mathbb{C}^{[B_m \times U]}$  corresponds to the part which is applied at BS  $m$ . Accordingly, each sub-matrix  $\bar{\mathbf{B}}_k \in \mathbb{C}^{[B \times U_k]}$  precodes the data of UE  $k$ , while the result is applied at all BSs. Linear precoding is in fact a filter operation that adapts the transmitted data to the current channel situation.

Due to regulations and technology constraints, each BS  $m$  needs to restrict its transmit power to  $\rho_m$  for each transmission block. For ease of notation, equal transmit power levels  $\rho_m = \rho, \forall m$  are assumed, while the precoding algorithms presented in this work can also

be applied for BS specific transmit power constraints. The block wise restriction results in the inequality

$$\mathbb{E}_{\mathbf{d}} \{ \text{tr}(\mathbf{B}_m \mathbf{d} \mathbf{d}^H \mathbf{B}_m^H) \} = \text{tr}(\mathbf{B}_m \mathbf{B}_m^H) \leq \rho, \quad (2.8)$$

for sufficiently large transmission blocks. The precoded symbol vector  $\mathbf{Bd}$  is transmitted over the multi-cell broadcast channel  $\mathbf{H} = [\mathbf{H}_1^T, \dots, \mathbf{H}_K^T]^T$ . Sub-matrix  $\mathbf{H}_k = [\mathbf{H}_{k,1}, \dots, \mathbf{H}_{k,M}]$  denotes the channel from all BSs to UE  $k$ , while  $\mathbf{H}_{k,m} \in \mathbb{C}^{[U_k \times B_m]}$  is the MIMO channel matrix between the antennas of BS  $m$  and UE  $k$ , respectively. It is assumed that the entries of  $\mathbf{H}$  are uncorrelated and the elements of  $\mathbf{H}_{k,m}$  are i.i.d. according to  $\text{vec}(\mathbf{H}_{k,m}) \sim \mathcal{N}_{\mathbb{C}}(\mathbf{0}, \lambda_{k,m} \mathbf{I})$ ,  $\forall k, m$ , resulting from a sufficiently high antenna separation [TV08].

The signal vector received at each UE  $k$  is impaired by additive white Gaussian noise (AWGN)  $\mathbf{n}_k \sim \mathcal{N}_{\mathbb{C}}(\mathbf{0}, \sigma_{n,k}^2 \mathbf{I})$  before it is equalized using the linear receive filter  $\mathbf{U}_k$ . Note that the noise power  $\sigma_{n,k}^2 = \sigma_n^2 + \sigma_{I,k}^2$  consists of receiver noise plus outer-cluster interference, as described in the previous section. The transmission equation is obtained by stacking the equalized data symbols of all  $K$  UEs into a single vector

$$\hat{\mathbf{d}} = \mathbf{U}(\mathbf{H}\mathbf{B}\mathbf{d} + \mathbf{n}) \quad (2.9)$$

where the receive filters of all UEs are collected in matrix  $\mathbf{U} = \text{blkdiag}(\mathbf{U}_1, \dots, \mathbf{U}_K)$  and  $\mathbf{n} = [\mathbf{n}_1^T, \dots, \mathbf{n}_K^T]^T$  is the overall noise vector. In addition, the precoded channel, which consists of the actual channel plus the precoding matrix is denoted by

$$\mathbf{T}_k = [\mathbf{T}_{k,1}, \dots, \mathbf{T}_{k,K}] = \mathbf{H}_k[\bar{\mathbf{B}}_1, \dots, \bar{\mathbf{B}}_K]. \quad (2.10)$$

The sub-matrix  $\mathbf{T}_{k,l}$  reflects the precoded channel between the data intended for UE  $l$  and the data received at UE  $k$  without noise.

### 2.2.1 Achievable Rate

A useful metric for evaluating the performance of a communication system is the data rate a user obtains on average. This refers to the average number of bits transmitted over a single channel use. The data rate, which each UE  $k$  can achieve at maximum by applying the precoding matrix  $\mathbf{B}$  reads

$$R_k = \log_2 \det(\mathbf{I} + \mathbf{\Pi}_k^{\text{S}}(\mathbf{\Pi}_k^{\text{I}})^{-1}), \quad (2.11)$$

where  $\mathbf{\Pi}_k^{\text{S}} = \mathbf{T}_{k,k} \mathbf{T}_{k,k}^H$  reflects the useful portion of the signal power, while  $\mathbf{\Pi}_k^{\text{I}} = \sum_{l \neq k} \mathbf{T}_{k,l} \mathbf{T}_{k,l}^H + \sigma_n^2 \mathbf{I}$  is the power of the remaining inter-user-interference plus noise. Equation (2.11) is based on the assumption that a coded bit block can be transmitted with  $R_k$  bits per channel use (bpcu), on average, while observing an infinitesimal error probability for decoding the block, if the block length goes to infinity [SW49, CT06].

An infinite block length is motivated by ensuring the observation of all possible noise realizations. Of course in practice, infinite block length is not achievable. Consequently,  $R_k$  can be achieved approximately by assuming a sufficiently large transmission block length  $L$ . Note that (2.11) does not refer to the capacity of the broadcast channel, since non-linear dirty paper coding [Cos83] instead of linear precoding would be required [CS03]. In addition to (2.11), the ergodic achievable rate is defined as the expectation w.r.t. the channel states  $\bar{R}_k = \mathbb{E}_{\mathbf{H}} \{R_k\}$ , while  $\bar{R} = 1/K \sum_{k=1}^K \bar{R}_k$  represents its average.

Assuming a fixed precoding matrix  $\mathbf{B}$ , the rate in (2.11) is only achievable under two conditions. First, the base station needs to know  $R_k$  in order to allocate this rate to the transmission block. For this purpose CSI needs to be available at the BS. Secondly, each UE  $k$  needs to have perfect knowledge of its own precoded channel  $\mathbf{T}_k$ , employing maximum likelihood (ML) reception. In the case of Gaussian distributed data symbols, as assumed in this work, ML reception corresponds to linear MMSE equalization filters  $\mathbf{U}_k$  in combination with successive interference cancellation (SIC) [TV08]. The next three sections refer to cases where these two conditions are not fulfilled.

### 2.2.2 Imperfect CSI at the Receiver

In general, CSIR is required in order to support coherent detection. Employing precoding with matrix  $\mathbf{B}$ , each UE  $k$  needs to know its precoded channel  $\mathbf{T}_k$ , which can be seen as an effective MIMO channel. If  $\mathbf{T}_k$  is only imperfectly known at the UE side, the useful signal portion in (2.11) is reduced due to incoherent detection effects [VSH06, MF11]. Accordingly, interference increases due to channel uncertainty. This effect can be modeled by interpreting the precoded channel known at the UE

$$\mathbf{T}_k = \hat{\mathbf{T}}_k + \boldsymbol{\Xi}_k, \quad (2.12)$$

as a random variable consisting of its estimate  $\hat{\mathbf{T}}_k = [\hat{\mathbf{T}}_{k,1}, \dots, \hat{\mathbf{T}}_{k,K}]$  and the random error matrix  $\boldsymbol{\Xi}_k = [\boldsymbol{\Xi}_{k,1}, \dots, \boldsymbol{\Xi}_{k,K}]$ . The error variance scales with the accuracy employed for signaling  $\mathbf{T}_k$  to the UE. Note, that a closed form expression of the error matrix distribution is typically hard to find. However, Gaussian approximations can be used to capture basic effects of forward signaling, as described in detail in Section 3.2.

Based on [MF11], the achievable rate in equation (2.11) is adapted by lowering the covariance of the useful signal portion  $\boldsymbol{\Pi}_k^S = \hat{\mathbf{T}}_{k,k} \hat{\mathbf{T}}_{k,k}^H$ , while the interference

$$\boldsymbol{\Pi}_k^I = \sum_{l \neq k} \hat{\mathbf{T}}_{k,l} \hat{\mathbf{T}}_{k,l}^H + \boldsymbol{\Xi}_k \boldsymbol{\Xi}_k^H + \sigma_n^2 \mathbf{I} \quad (2.13)$$

is increased by the uncertainty  $\boldsymbol{\Xi}_k \boldsymbol{\Xi}_k^H$ , which can be interpreted as additional noise.

### 2.2.3 Imperfect CSI at the Transmitter

As already mentioned in Section 2.2.1, CSIT needs to be available in order to allocate the transmission rate which is achievable for the current channel  $\mathbf{H}$  in combination with the precoding matrix  $\mathbf{B}$  applied. The aspect of imperfect rate allocation is discussed in Section 2.2.4 in greater detail.

The primary concern, which is a focus of this section, is the adjustment of the precoding matrix under imperfect CSIT conditions. A detailed model of the effects which lead to impaired CSIT is given in Section 2.3, while minimizing its impact is the main issue in Section 3.1. In this section, the impairment details are neglected and imperfect CSIT of the link between BS  $m$  and UE  $k$  is expressed by the error variance  $\epsilon_{k,m}$ .

Similar to the imperfect CSIR model, the actual channel known at the transmitter side can be interpreted as random variable

$$\mathbf{H} = \hat{\mathbf{H}} + \mathbf{E}, \quad (2.14)$$

where the CSI matrix  $\hat{\mathbf{H}} = [\hat{\mathbf{H}}_1^T, \dots, \hat{\mathbf{H}}_K^T]^T$  with  $\hat{\mathbf{H}}_k = [\hat{\mathbf{H}}_{k,1}, \dots, \hat{\mathbf{H}}_{k,M}]$  is uncorrelated with the Gaussian error matrix  $\mathbf{E} = [\mathbf{E}_1^T, \dots, \mathbf{E}_K^T]^T$  with  $\mathbf{E}_k = [\mathbf{E}_{k,1}, \dots, \mathbf{E}_{k,M}]$  and  $\text{vec}(\mathbf{E}_{k,m}) \sim \mathcal{N}_{\mathbb{C}}(\mathbf{0}, \epsilon_{k,m}\mathbf{I})$ . Note that the error variances  $\epsilon_{k,m}$  of each BS-UE link are potentially different due to independent mean channel gains  $\lambda_{k,m}$ , while the elements of  $\mathbf{E}_{k,m}$  have equal variances due to the same statistics in all sub-links of a certain BS-UE link.

Note that, (2.14) as well as (2.12) follow from the assumption that CSI is obtained by employing MMSE estimation [Kay93]. Otherwise, the model need to be extended by additionally scaling the estimate.

For processing the precoding matrix, it is assumed that there is a common estimate  $\hat{\mathbf{H}}$  available at the CN, while each individual BS  $l$  sees a different estimate  $\hat{\mathbf{H}}\langle l \rangle$ , which is potentially not perfectly known at the other BSs, due to, e.g., backhauling issues. In order to model the aspect of different versions of estimates,

$$\mathbf{H} = \hat{\mathbf{H}}\langle l \rangle + \mathbf{E}\langle l \rangle \quad (2.15)$$

need to hold at each individual BS  $l$ . Note that,  $\hat{\mathbf{H}}\langle l \rangle$  is equivalent at all BSs, if the backhaul is perfect (no latency or capacity issues). On the other hand, completely uncorrelated estimates can be available at the BSs, if the backhaul introduces tremendously large delays.

The error variances  $\mathbf{\Gamma} = [\epsilon_1, \dots, \epsilon_M]$ , with  $\epsilon_m = [\epsilon_{1,m}, \dots, \epsilon_{K,m}]^T$  seen at the CN, as well as the BS-wise variances  $\mathbf{\Gamma}\langle l \rangle$  are perfectly known to every entity of the system, which follows from the basic assumption regarding long term statistics in this thesis.

### 2.2.4 Rate with Outage

The rate which is assigned for transmission is calculated based on CSIT and the respective precoding matrix. If CSIT is impaired, the channel assumed for the rate calculation differs from the actual channel. In the following,  $\hat{R}_k$  refers to the rate which is computed from (2.11) with imperfect CSIT  $\hat{\mathbf{H}}$ . In case the assigned rate is smaller than the rate  $R_k$  which could be transmitted over the actual channel, the potential of the channel state is not exploited completely. In contrast, if the actual channel does not support the assigned rate, the transmitted block cannot be decoded with infinitesimal error probability as stated in Section 2.2.1. In this case, outage occurs.

In this work, only full outage is considered which refers to retransmitting the whole block if it cannot be decoded in the first place. In contrast, hybrid automatic repeat request (H-ARQ) only requires transmitting additional incremental information required for decoding the data block. Assuming ideal H-ARQ, the full rate  $R_k$  can be achieved asymptotically by always transmitting more information than supported by the channel.

Therefore, the two corner cases of rate without outage and rate with full outage are considered in this work. The actual rate of a practical system lies somewhere in between. For the case of full outage, the rate actually assigned can be adjusted by introducing a back-off factor  $\psi_k$  and assigning the rate  $\psi_k \hat{R}_k$  for transmission. The probability of outage reads

$$p_{\text{out},k} = \Pr \left( R_k < \psi_k \hat{R}_k \right). \quad (2.16)$$

The rate actually transmitted (on average) results in

$$\bar{R}_{\text{out},k} = (1 - p_{\text{out},k}) \cdot \psi_k \mathbb{E}_{\mathbf{H}} \left\{ \hat{R}_k \right\}. \quad (2.17)$$

The rate in (2.17) refers to the product of the probability that the transmitted block can be decoded correctly and the transmission rate assigned on average. In order to improve the net rate  $\bar{R}_{\text{out},k}$ , the back-off factor can be optimized. Note, that more advanced rate assignment schemes can include a finite number of H-ARQ rounds, as described in [WJ10, KCBS11].

### 2.2.5 Basic Precoding Strategies

One of the fundamental methods in linear multiuser-MIMO precoding is zero-forcing (ZF) [JKG<sup>+</sup>02]. The aim of ZF is to completely cancel the interference between data streams transmitted in parallel by multiplying the data vector with a scaled version of the channel's pseudo inverse

$$\mathbf{B} = \tilde{\mathbf{B}}\mathbf{P} = \left[ \tilde{\mathbf{B}}_1, \dots, \tilde{\mathbf{B}}_M \right] \mathbf{P} = \mathbf{H}^H (\mathbf{H}\mathbf{H}^H)^{-1} \mathbf{P}. \quad (2.18)$$

The multiplication with matrix  $\mathbf{P}$  handles two major issues. The first one is to satisfy the transmit power constraint for each BS. This can be achieved by calculating a scaling

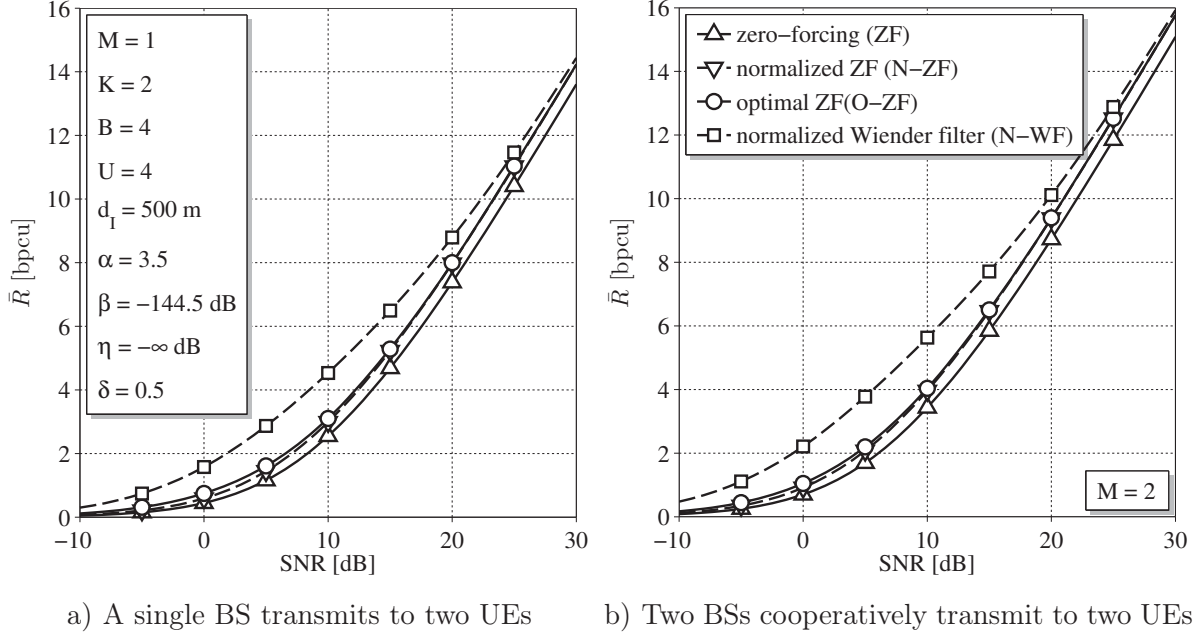


**Fig. 2.4:** Ergodic achievable rate performance as a function of the cell edge SNR for four basic precoding algorithms under perfect CSI conditions.

factor

$$b = \min_m \left\{ \rho / \text{tr} \left( \tilde{\mathbf{B}}_m \tilde{\mathbf{B}}_m^H \right) \right\} \quad (2.19)$$

which is multiplied with an identity matrix to obtain  $\mathbf{P} = b\mathbf{I}$ . Note that according to (2.19), only a single BS transmits with full power  $\rho$ . The second constraint for designing matrix  $\mathbf{P}$  is the allocation of the total transmit power to the different data streams. This is advantageous for sum rate optimization since stronger channels can contribute more to the overall performance rate. An easy solution is to normalize the columns of  $\tilde{\mathbf{B}}$  in order to transmit each data stream with the same overall power instead of achieving the same received power at each UE antenna [PHG09]. This precoding method is denoted as normalized ZF (N-ZF). The corresponding matrix reads

$$\mathbf{P} = b \cdot \text{dg} \left( \tilde{\mathbf{B}}^H \tilde{\mathbf{B}} \right)^{-1} = b \cdot \left[ \check{\mathbf{B}}_1, \dots, \check{\mathbf{B}}_M \right], \quad (2.20)$$

where the linear scaling with  $b$  is done according to (2.19) by replacing  $\tilde{\mathbf{B}}_m$  with  $\check{\mathbf{B}}_m$ . The rate maximizing power allocation strategy for ZF precoding is water-filling [YG06], where channels which are weaker than a certain water level are deactivated completely and no power is allocated to the respective data stream. Since this ZF strategy is optimal in terms of rate, it is denoted as optimal ZF (O-ZF).

The disadvantage of ZF is that in order to achieve the complete cancellation of inter-stream interference, a considerable amount of signal power is radiated in directions where it is not used. As a result, the signal strength received at the UE is weak, which is especially critical if the SNR is low. In contrast, precoding with the Wiener filter (WF) approach

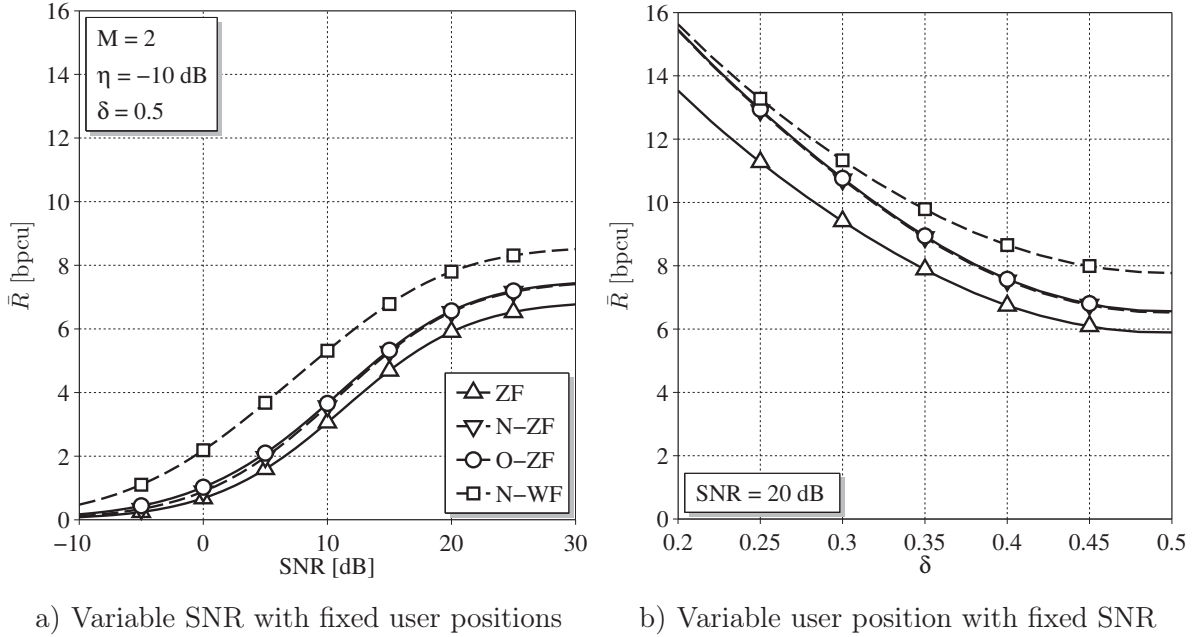


**Fig. 2.5:** Ergodic achievable rate performance including inter-cluster interference under perfect CSI conditions.

takes the noise power into account [DHJU03a]. The solution follows from minimizing the MSE between the data symbol vector  $\mathbf{d}$  actual transmitted and its estimate  $\hat{\mathbf{d}}$ , while it includes an additional regularization term within the pseudo inverse of the channel. The overall precoding matrix results in

$$\mathbf{B} = \tilde{\mathbf{B}}\mathbf{P} = [\tilde{\mathbf{B}}_1, \dots, \tilde{\mathbf{B}}_M]\mathbf{P} = (\mathbf{H}^H\mathbf{H} + \sigma_n^2\mathbf{I})^{-1}\mathbf{H}^H\mathbf{P}. \quad (2.21)$$

Scaling with the diagonal matrix  $\mathbf{P}$  can be done by normalizing the columns of  $\tilde{\mathbf{B}}$ , denoted as normalized WF (N-WF). However, finding the rate optimal power allocation strategy is not trivial, since  $\mathbf{P}$  scales both the useful signal and the interference between data streams. A solution which exploits uplink-downlink duality was given in [SSB07].

Fig. 2.4 illustrates the average ergodic achievable rate  $\bar{R}$  as a function of the SNR for the four precoding schemes mentioned before, where inter-cluster interference is not taken into account. Utilizing the urban macro-cell scenario in [Tec10], the ISD is determined to be  $d_I = 500$  m, and  $\beta = -144.5$  dB. The left plot refers to a setup with a single BS with  $B = 4$  transmit antennas and two UEs both equipped with two antennas, resulting in the overall number of  $U = 4$  antennas. Both users are located at  $d_{k,1} = d_I/2, \forall k$  away from the BS, resulting in  $\delta = 0.5$ . The power allocation of N-ZF is independent of the SNR which results in a constant performance gain compared to ZF for the high SNR regime. This follows from the double-logarithmic relation between rate and SNR which behaves linearly for higher values. The advantage of O-ZF is the possibility of deactivating data streams if the corresponding channels falls below a certain water level, which scales with the SNR. Without considering deactivation, N-ZF is equivalent to O-ZF. Fig. 2.4 shows that O-ZF

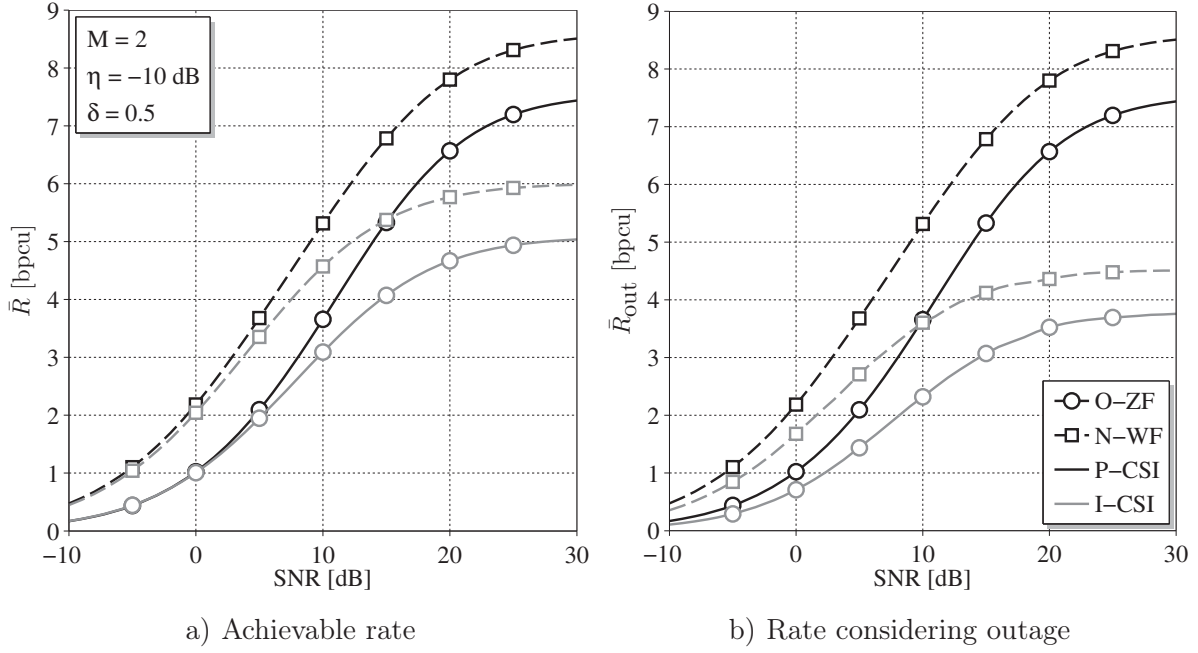


**Fig. 2.6:** Ergodic achievable rate performance including inter-cluster interference under imperfect CSI conditions.

outperforms N-ZF in the low SNR regime, where the deactivation of data streams is more likely. Incorporating the noise power into the precoding scheme, as in N-WF, leads to additional performance gains due to the higher received power. With increasing SNR, the regularization within the pseudo inverse disappears and the performance converges towards the N-ZF solution.

The basic behavior for the case of  $M = 2$  serving BSs, each equipped with  $B_m = 2$  antennas is similar to the single BS setup, as illustrated in Fig. 2.4 b). Since the overall number of transmit antennas  $B$  is constant, the maximum number of parallel data streams possible does not change. Regarding a certain SNR point (which refers to specific transmit power per BS proportional to a certain noise power), the transmit power allowed is doubled compared to the single BS case. As a result, the curves are shifted to the left. However, the shift is smaller than 3 dB because only one BS exploits the full transmit power  $\rho$ , resulting from consistent scaling according to (2.19). Note that, allowing interference between data streams, inconsistent scaling can be beneficial for improving the rate performance. Further discussions on that issue follow in Chapter 4.

Taking inter-cluster interference into account by adjusting  $\sigma_{n,k}^2, \forall k$  accordingly, results in a rate saturation in the high SNR regime as seen in Fig. 2.5 a). In this case the performance gains of N-WF are significant for the whole SNR range. This effect results from the saturation of the SINR (see Section 2.1.1), which directly influences the achievable rate.

Fig. 2.5 b) shows the rate performance over the relative user distance  $\delta$ , assuming a cell edge SNR of 20 dB, which is close to the saturation point. Operating at an SNR which is little affected by the saturation (10 - 20 dB) would be appropriate from an energy

efficiency point of view. Moving the UEs closer to their local BSs lead to a increased SINR as discussed in Section 2.1.1. Consequently, the rate performance behavior is similar to the high SNR regions without inter-cluster interference. Fig. 2.5 b) shows, that the performance gap between N-WF and N-ZF/O-ZF gets smaller with decreasing  $\delta$ . The same can be observed in Fig. 2.4 b) for large SNRs.

### Precoding with Imperfect CSIT

When CSI is only imperfectly available at the BS side, the precoding matrix is not perfectly aligned with the actual MIMO channel. Computing  $\mathbf{B}$  according to the precoding algorithms introduced, where the actual channel  $\mathbf{H}$  is replaced by its estimate  $\hat{\mathbf{H}}$  results in substantial data rate losses in the high SNR regime. Fig. 2.6 illustrates the performance for imperfect CSI (I-CSI) and perfect CSI (P-CSI). The left plot a) shows the achievable rate according to (2.11), where 1 bpcu is already lost at SNR = 15 dB if the CSIT is impaired with  $\epsilon = 0.1 \cdot \lambda$ . Considering full outage (no H-ARQ) with an optimized back-off factor  $\psi_k, \forall k$  as shown in Fig. 2.6 b), results in about 2 bpcu rate loss compared to perfect CSI. In addition, the rate loss is more significant even in the low SNR regime.

## 2.3 Feedback Signaling

As explained in the previous sections, precoding requires CSI to be available at the BS side. In this work, an FDD system is assumed where the downlink channel cannot be measured from uplink pilots and CSI is fed back via uplink transmission. This section introduces a mathematical model for imperfect CSI based on several impairment sources. Furthermore, the application to cooperative scenarios with DP is given.

### 2.3.1 CSI Feedback Chain

The process between measuring CSI from downlink pilots to its availability at the BS is illustrated in Fig. 2.7, taking into account that CSI is impaired by noisy pilot reception, quantization, and delays. In the following,  $h[t, f] \sim \mathcal{N}_{\mathbb{C}}(0, \lambda)$  denotes an instance of the i.i.d. channel coefficients related to a certain BS-UE connection, where indices for antennas at transmitter and receiver side are omitted for readability. Furthermore,  $t$  and  $f$  denote the transmission block index in time and frequency, respectively.

#### Noisy Pilot Reception

In order to observe the downlink channel, the BSs transmit pilot signals which are known at the UEs. Within a transmission block, each BS antenna occupies  $N_P$  channel uses with pilot signals. The transmit power  $\rho$  is assumed to be equivalent to the power used for data

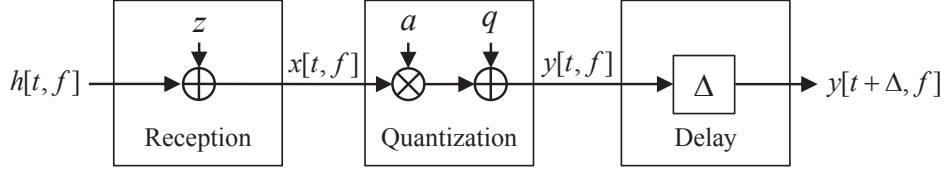


**Fig. 2.7:** Feedback model for reporting CSI back to the transmitter side.

transmission. Since pilots from different BS antennas use orthogonal resources, the pilot density results in  $\varrho_P = BN_P/L$ .

According to the downlink model in Section 2.2, the received signals are corrupted by Gaussian noise with variance  $\sigma_n^2$ . The scaled model assuming unit pilot signals results in

$$x[t, f] = h[t, f] + z, \quad (2.22)$$

with Gaussian noise  $z \sim \mathcal{N}_{\mathbb{C}}(0, \sigma_z^2)$  and noise variance  $\sigma_z^2 = \sigma_n^2/(N_P \rho)$  reflecting the combination of  $N_P$  observations experiencing the same channel state. Note that each of the  $N_P$  pilots experiences a different noise realization.

## Quantization

The noisy channel observations need to be fed back to the transmitter for computing the precoding matrix. Since the feedback rate is limited, each coefficient is quantized with  $Q$  bits. Under the assumption of a large number of i.i.d. channel coefficients, the distortion due to quantization can be lower bounded with rate distortion theory [CT06]. This assumption is motivated by spatially uncorrelated links for each BS-UE connection in combination with carrier aggregation, where a UE gets resources from different parts of the spectrum which are uncorrelated in frequency. An adaptation of the original rate distortion model was presented in [FOF13b].

Based on channel coefficients  $h[t, f] \sim \mathcal{N}_{\mathbb{C}}(0, \lambda)$  and receiver noise  $z \sim \mathcal{N}_{\mathbb{C}}(0, \sigma_z^2)$ , the input of the quantizer (2.22) is also Gaussian distributed  $x[t, f] \sim \mathcal{N}_{\mathbb{C}}(0, \sigma_x^2)$  with variance  $\sigma_x^2 = \lambda + \sigma_z^2$ . The relation between  $x[t, f]$  and quantizer output  $y[t, f]$  results in

$$y[t, f] = ax[t, f] + q, \quad (2.23)$$

where  $a = 1 - 2^{-Q}$  scales the quantizer input before it is distorted by quantization noise  $q \sim \mathcal{N}_{\mathbb{C}}(0, \sigma_q^2)$ , which is uncorrelated to  $x[t, f]$ . In the original model, quantizer input and quantization noise are dependent. The dependence can be eliminated with scalar  $a$  and the variance of the independent noise

$$\sigma_q^2 = 2^{-Q}(1 - 2^{-Q})\sigma_x^2. \quad (2.24)$$

A detailed derivation is given in Appendix A.

### Outdated CSI

Outdated CSI is modeled based on the correlation between two delayed coefficients of a time-variant channel, which result from mobile UEs, moving with velocity  $v$ . Based on Jakes Doppler spectrum and the normalized delay  $\Delta_t$ , the correlation is

$$\mathbb{E} \{h[t, f]h^*[t \pm \Delta_t, f]\} = c[\Delta_t] = J_0 \left( 2\pi \frac{L_t f_C v}{f_s v_c} \Delta_t \right) \lambda, \quad (2.25)$$

where  $f_C$ ,  $f_s$ ,  $v_c$  and  $J_0$  are the carrier frequency, the sample frequency, the speed of light, and the zero-th order Bessel function of the first kind, respectively.

### Combined Feedback Model

All three impairments are combined to a single equation. The channel observed at the BS with delay  $\Delta_t$  is

$$y[t, f] = a(h[t - \Delta_t, f] + z) + q. \quad (2.26)$$

A measure of channel uncertainty at the BS is given by the MSE between the actual channel  $h[t]$  and the CSI in (2.26), as

$$\begin{aligned} \epsilon &= \mathbb{E} \{|h[t, f] - y[t, f]|^2\} \\ &= \lambda - 2ac[\Delta_t] + a^2(\lambda + \sigma_z^2) + \sigma_q^2 \\ &= \lambda + a(\lambda + \sigma_z^2 - 2c[\Delta_t]). \end{aligned} \quad (2.27)$$

The third line in (2.27) is obtained by substituting (2.24). Note that for the MSE in (2.27), no channel prediction is performed and the observations  $y[t, f]$  are directly used as CSI  $\hat{h}$ . How to improve CSI quality by channel prediction is described in Section 3.1.1.

### 2.3.2 Simplified CSI Model

The model in (2.26) is not convenient to handle since it includes a dependence between the actual channel  $h[t + \Delta, f]$  and its estimate  $\hat{h}[t, f] = y[t, f]$  at different time instances, while a dependence at the same time instance  $t$  is preferred. In order to achieve a simplified representation, the model can be rewritten as

$$\hat{h}[t, f] = vh[t, f] + \hat{e}, \quad (2.28)$$

where  $v \in \mathbb{R}_+$  is a real scalar and  $\hat{e} \sim \mathcal{N}_C(0, \Omega)$  refers to AWGN. Note that the rewritten model in (2.28) results in the same channel uncertainty as in (2.27) but without carrying along channel states at multiple time instances. The parameters  $v$  and  $\Omega$  of the transformed model can be derived by ensuring that the correlation  $\mathbb{E}\{h[t, f]\hat{h}^*[t, f]\}$  as well as

the variance of the CSI  $\mathbb{E}\{|\hat{h}[t, f]|^2\}$  are equal in both models, which gives

$$\begin{aligned} \mathbb{E}\{h[t, f]\hat{h}^*[t, f]\} &\stackrel{\text{from (2.26)}}{=} ac[\Delta_t] \\ &\stackrel{\text{from (2.28)}}{=} v\lambda, \end{aligned} \quad (2.29)$$

resulting in the  $v = ac[\Delta_t]/\lambda$ . The variance  $\Omega$  is obtained by calculating

$$\begin{aligned} \mathbb{E}\{|\hat{h}[t, f]|^2\} &\stackrel{\text{from (2.26)}}{=} a^2(\lambda + \sigma_z^2) + \sigma_q^2 \\ &\stackrel{\text{from (2.28)}}{=} v^2\lambda + \Omega. \end{aligned} \quad (2.30)$$

Inserting (2.24) and rearranging (2.30) results in the variance  $\Omega = a(\lambda + \sigma_z^2 - c^2[\Delta_t]/\lambda)$ . Extending the simplified model to the complete multi-cell broadcast channel results in

$$\hat{\mathbf{H}}_{k,m} = v_{k,m}\mathbf{H}_{k,m} + \hat{\mathbf{E}}_{k,m}, \quad (2.31)$$

where the noise matrix  $\hat{\mathbf{E}}_{k,m}$  has uncorrelated elements according to  $\text{vec}(\hat{\mathbf{E}}_{k,m}) \sim \mathcal{N}_{\mathbb{C}}(\mathbf{0}, \Omega_{k,m}\mathbf{I})$ .

### 2.3.3 CSI in Distributed Setups

The model in (2.28) is applied to distributed setups where the same CSI is used at multiple BSs. Taking into account that transmission over the backhaul is affected by latency, the local BS receives the same CSI version with a smaller delay than all remote BSs to whom the CSI is forwarded via the backhaul, leading to inconsistent CSI versions at the BSs. The quantities  $\Omega_{k,m}\langle l \rangle$  and  $v_{k,m}\langle l \rangle$  depend on the BS  $l$  where the CSI is available. Since backhaul transmission cannot improve CSI quality, the local BS at least has the same CSI accuracy of its UEs when compared to the remote BSs. The CSI of the link  $k, m$  which is available at BS  $l$  is defined as:

$$\hat{\mathbf{H}}_{k,m}\langle l \rangle = \begin{cases} v_{k,m}\langle l \rangle\mathbf{H}_{k,m} + \hat{\mathbf{E}}_{k,m}\langle l \rangle & \text{if } k \in \mathcal{K}_l \\ v_{k,m}\langle l \rangle\mathbf{H}_{k,m} + \bar{\mathbf{E}}_{k,m}\langle l, n \rangle & \text{if } k \in \mathcal{K}_n, \forall n \neq l. \end{cases} \quad (2.32)$$

The noise matrix  $\bar{\mathbf{E}}_{k,m}\langle l, n \rangle = \hat{\mathbf{E}}_{k,m}\langle n \rangle + \hat{\mathbf{E}}_{k,m}\langle l, n \rangle$  consists of the error matrix  $\hat{\mathbf{E}}_{k,m}\langle n \rangle$  due to feedback transmission to BS  $n$  and the additional error matrix  $\hat{\mathbf{E}}_{k,m}\langle l, n \rangle$  referring to the impairment resulting from backhaul forwarding from BS  $n$  to BS  $l$ , where  $\text{vec}(\hat{\mathbf{E}}_{k,m}\langle l, n \rangle) \sim \mathcal{N}_{\mathbb{C}}(\mathbf{0}, \Omega_{k,m}\langle l \rangle - \Omega_{k,m}\langle n \rangle\mathbf{I})$ .